

Phosphorescence properties and chiral discrimination of camphorquinone enantiomers in the presence of α -cyclodextrin and 1,2-dibromoethane

Yu Wang^{a,*}, Tingting Feng^a, Jianbin Chao^a, Liping Qin^a, Zhao Zhang^a, Weijun Jin^{b,**}

^a School of Chemistry and Chemical Engineering, Shanxi University, Taiyuan 030006, China

^b College of Chemistry, Beijing Normal University, Beijing 100875, China

ARTICLE INFO

Article history:

Received 25 December 2009

Received in revised form 9 March 2010

Accepted 28 March 2010

Available online 3 April 2010

Keywords:

Camphorquinone

Room temperature phosphorescence

Lifetime

Chiral discrimination

ABSTRACT

Strong room temperature phosphorescence (RTP) of camphorquinone (CQ) is synergistically induced by α -cyclodextrin (α -CD) and 1,2-dibromoethane (1,2-DBE) without removal of oxygen dissolved in the solution because of the formation of ternary complex of α -CD, CQ, and 1,2-DBE. Both (R)-CQ and (S)-CQ exhibit single exponential phosphorescence decay with lifetimes of (0.274 ± 0.014) and (0.639 ± 0.021) ms for (R)-CQ and (S)-CQ, respectively. The relatively large RTP lifetime difference observed for (R)-CQ and (S)-CQ enables easy spectroscopic discrimination between this pair of enantiomers. The apparent association constant of (S)-CQ/1,2-DBE/ α -CD complex is larger than that of (R)-CQ/1,2-DBE/ α -CD complex, implying that the former ternary complex should consist of an optimal arrangement of components. ^1H NMR as well as 2D NMR spectroscopy has been used to study the inclusion complexation of α -cyclodextrin with CQ in order to understand the binding model.

© 2010 Elsevier B.V. All rights reserved.

1. Introduction

Chiral recognition, as an aspect of molecular recognition, has been a subject of great interest in pharmaceutical and many other related fields. There are currently several analytical techniques used for the chiral discrimination, including microcalorimetry, circular dichroism, mass spectrometry, NMR, spectroscopy and various chromatographic methods [1–8]. Enantioselective receptor–substrate interactions form the basis of chiral recognition. Cyclodextrins are among the most commonly used supramolecular receptors that recognize the chiral guest molecules [9–13]. Possessing chiral hydrophobic cavities, these macrocycles are inherently dissymmetric and are thus able to distinguish between stereochemical isomers due to the formation of diastereomeric host–guest complexes with different interactions for each enantiomer.

In recent years, room temperature phosphorimetry has been employed for the chiral analysis of diastereomers/enantiomers due to its large Stokes shift, high sensitivity, good selectivity and especially longer and easily measurable triplet lifetimes [14–20]. Upon complexation of phosphorescent chiral analytes with CDs, different RTP intensity and lifetimes are obtained for the analyte enantiomers. Thus, RTP induced by cyclodextrin (CD-RTP),

first introduced by Cline Love and co-worker [21] in 1984, can be used for enantioselective analysis. In previous studies, we have investigated the chiral discrimination of quinine and quinidine as well as (R) and (S)-1,1'-binaphthol by room temperature phosphorimetry, using γ -CD as a chiral selector [18,19]. In the present paper we continue our work on the enantiomeric phosphorescence detection of camphorquinone (CQ), a chiral α -diketone. Owing to its spectral characteristics such as a long triplet lifetime in solution at room temperature, a high intersystem crossing yield and long-wavelength singlet absorption, CQ has been frequently used as a photosensitizer for dental resin composites and as a photoinitiator for light cured resin compositions [22,23]. A spectroscopic and photophysical study on the chiral discrimination of camphorquinone enantiomers by cyclodextrins had been reported earlier in the literature [3]. More recently, α -CD was used to discriminate between (R)- and (S)-CQ based on differences in RTP lifetimes [16]. In this study, the RTP of CQ in CDs solution was reported for the first time. However, the observation of RTP required removal of the dissolved oxygen from solutions by nitrogen purging, which is a time-consuming process and produces some inconveniences. Moreover, the resultant RTP signals were relatively weak and noisy so that high precision level could not be achieved. We report here a detailed study of the RTP of CQ synergistically induced by α -cyclodextrin and a third component as a space-regulator without deoxygenation. The observed larger RTP intensity and lifetime differences are used to investigate the chiral recognition of CQ. In addition, we obtain the corresponding NMR results to elucidate the complexation of CQ with α -CD.

* Corresponding author. Tel.: +86 351 7010319; fax: +86 351 7011688.

** Corresponding author. Tel.: +86 1 58802146; fax: +86 1 58802146.

E-mail addresses: wangyu1168@sxu.edu.cn (Y. Wang), wjjin@bnu.edu.cn (W. Jin).

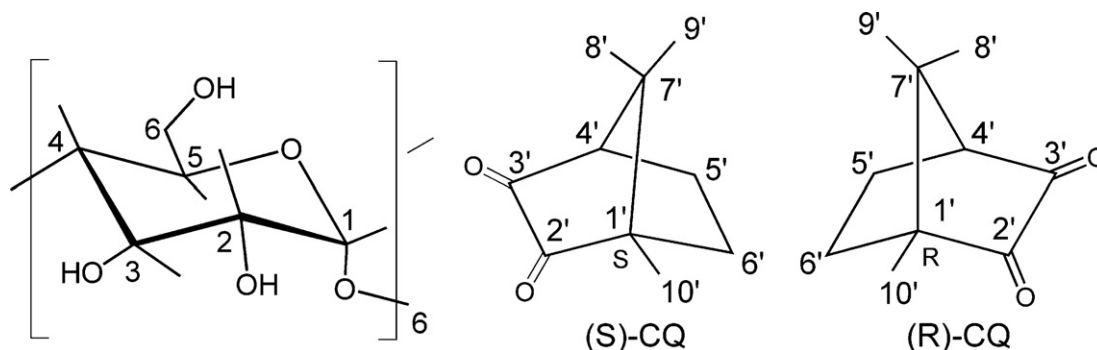


Chart 1. Left: numbering of carbon atoms in the α -CD glucopyranose residue. Right: Structures and ring numbering conventions for (R)-CQ and (S)-CQ.

2. Experimental

2.1. Reagents

(1R)-(-)-camphorquinone ((R)-CQ) and (1S)-(+)-camphorquinone ((S)-CQ), as shown in Chart 1, were purchased from Alfa Aesar (Lancaster, UK). α -CD, β -CD and γ -CD were obtained from Wacker Co. (Munich, Germany) and used as received. Absolute ethyl alcohol ($\geq 99.7\%$), 1,2-dibromoethane (1,2-DBE), 1,4-dibromobutane (1,4-DBB), butyl iodide (IBu), bromocyclohexane (BrCH), 1,2,3-tribromopropane (1,2,3-TBP), 1,2-dibromopropane (1,2-DBP) and dibromomethane (DBM) ($\geq 98.0\%$) were purchased from Beijing Chemicals Factory (Beijing, China). Stock solutions of (R)-CQ and (S)-CQ were prepared in ethanol at $1.0 \times 10^{-1} \text{ mol L}^{-1}$. Doubly distilled water was used throughout.

2.2. Apparatus

The UV absorption experiments were carried out on TU-1901 spectrophotometer (Puxi instrument Co., Beijing, China). Phosphorescence intensity measurements were performed on LS-55 Luminescence Spectrometer (PerkinElmer, Beaconsfield, UK). The samples were excited at 475 nm and the phosphorescence signal was monitored at 562 nm. The excitation and emission slits were set at 10 and 20 nm, respectively. The delay time and the gate width were set at 0.05 and 2 ms, respectively. Phosphorescence lifetimes were determined with Cary Eclipse Fluorescence Spectrophotometer (Varian, Palo Alto, USA). The first delay time was set at 0.1 ms while the gate time was set at 0.05 ms. The phosphorescence lifetime values were obtained by fitting the RTP decay curves to single- or biexponential curve.

All one-dimensional ^1H NMR spectra were recorded on a DRX-300 spectrometer (Fällenden, Switzerland). To achieve a suitable solubilization of both CQ and α -CD, a binary solvent of deuterated acetone and D_2O (1:20, v/v) was used for the NMR measurements. And the ROSEY spectroscopy of CQ/ α -CD complex was conducted at 25°C .

Molecular modeling software (CS Chem3D Version 8.0, MM2) was used to optimize the conformation of the CQ/1,2-DBE/ α -CD complex.

2.3. Procedures

Typically, appropriate amount of stock solutions of (R)-CQ and (S)-CQ was transferred into a comparison tube of 10 ml, and then proper volumes of α -CD and 1,2-DBE solution were added. The mixed solution was diluted to the final 5 ml with doubly distilled water and shaken thoroughly. The working solutions were left to equilibrate for 1 h at room temperature before making measure-

ments. Enantiomeric mixtures of CQ were made by mixing known amounts of single enantiomeric stock solutions by weight. All the other CD systems follow the same procedure.

3. Results and discussion

3.1. Absorption and luminescent spectra

The band at 454 nm is attributed to a $n-\pi^*$ transition in the absorption spectra of CQ (data not shown for the sake of brevity). As previously reported [24], CQ shows low absorptivity. Addition of α -CD to the aqueous solution of CQ resulted in an increase in the absorbance and a red shift of ca. 5 nm from 454 to 459 nm, indicating that the CQ molecules are included into the hydrophobic cavity of CD. The band at shorter wavelength also exhibited red shift upon addition of CD although the exact absorption peak is not discernable. The absorption changes are very similar for both R and S enantiomer.

Fluorimetric measurements were also performed in aqueous solutions of α -CD. The fluorescence spectrum of (R)-CQ is very similar to that of (S)-CQ with respect to position and relative intensity. The difference in fluorescence emission intensity of the peak at 500 nm was too small to be used for chiral discrimination.

In aqueous solutions of CDs, CQ was found to give intense RTP emissions without deoxygenation in the presence of the third component such as 1,2-DBE. The observed RTP can be attributed to the formation of a ternary complex, namely, CDs/CQ/1,2-DBE. Herein 1,2-DBE acts as both space-regulator and heavy atom perturber. As a space-regulator, 1,2-DBE inserts into the cavity of CDs and contributes to the formation of a tight ternary complex, which suppress diffusion of triplet state quenchers, such as molecular oxygen, and restrict the internal motions of the phosphorescent molecule. CQ is thus experiencing a sufficiently rigid microenvironment to produce strong RTP emission. As a heavy atom perturber, 1,2-DBE can enhance the probability of $S_1 \rightarrow T_1$ intersystem crossing and induce strong phosphorescence.

As shown in Fig. 1, all three CDs (α -CD, β -CD and γ -CD) can induce CQ to emit strong RTP in the presence of 1,2-DBE. However, no remarkable differences in the RTP intensity were observed for (R)-CQ and (S)-CQ in the case of β -CD and γ -CD (Fig. 1 inset). By contrast, significant discrimination was observed for the α -CD inclusion, indicating that α -CD is the best host for chiral recognition of CQ. Fig. 2 shows the RTP spectra of (R)-CQ and (S)-CQ in the presence of α -CD. The emission of both enantiomers is peaked at 562 nm. The RTP intensity of (S)-CQ was greater than that of (R)-CQ, the difference being 61.1%. Thus, it can be inferred that (S)-CQ in its triplet state is much better protected from quenching than (R)-CQ. According to the so-called three-point interaction model between one enantiomer and the chiral selector [25], the interaction between the chiral α -CD cavity and CQ may be modified by

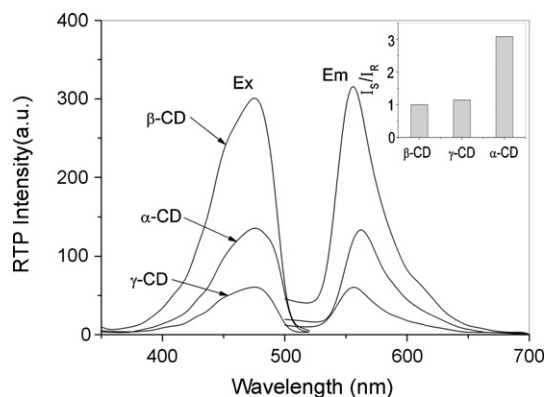


Fig. 1. Phosphorescence spectra of (R)-CQ in different cyclodextrins. ($[(R)\text{-CQ}] = 1.0 \times 10^{-3} \text{ mol L}^{-1}$; $[\text{CDs}] = 8.0 \times 10^{-3} \text{ mol L}^{-1}$; $V_{1,2\text{-DBE}} = 6 \mu\text{L}$ in 5 mL) Inset: the ratio of RTP intensity of (S)-CQ to (R)-CQ.

1,2-DBE to achieve a better fit and a stronger interaction, which further enlarges the spectra gap in chiral recognition. As the solution became turbid in the presence of 1,2-DBE, the measurements of either absorption or fluorescence spectra are difficult or impossible because of the strong scattering of the light. For such systems, the phosphorimetric technique presents special advantages over the other spectroscopic methods.

3.2. Optimization of phosphorescence measurement conditions

3.2.1. Screening of heavy atom perturbers

Some haloalkanes (1,4-DBB, DBM, 1,2-DBP, BrCH₃, 1,2,3-TBP, IBu and 1,2-DBE) were investigated as heavy atom perturbers (HAP). As shown in Fig. 3, all the haloalkanes tested can induce RTP of CQ in α -CD solution but to a different degree. Among the haloalkanes tested, 1,2-DBE not only showed the most intense RTP signals but also displayed a high level of enantioselectivity. After considering the aspects in both sensitivity and enantioselectivity, 1,2-DBE was selected to discriminate the enantiomers of CQ in this work.

3.2.2. Selection of both α -CD and 1,2-DBE concentrations

The phosphorescence intensity of the included CQ was found to depend on the concentration of the heavy atom moiety and on the concentration of α -CD. As shown in Fig. 4, in the presence of 1,2-DBE, the RTP intensity of CQ increased sharply with the increase of α -CD concentration. This change became slow and finally reached a plateau when the concentration of CD was more than 16 mM, indicating that the stable inclusion occurs among CQ, α -CD, and 1,2-DBE. A suitable α -CD concentration of 0.02 M was chosen for all the subsequent experiments.

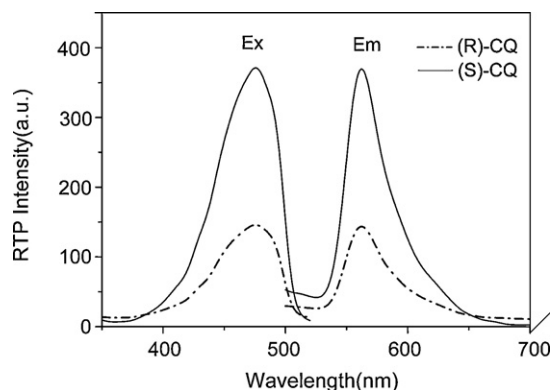


Fig. 2. Phosphorescence spectra of CQ in α -CD solution. ($[\text{CQ}] = 1.0 \times 10^{-3} \text{ mol L}^{-1}$; $[\alpha\text{-CD}] = 2.0 \times 10^{-2} \text{ mol L}^{-1}$; $V_{1,2\text{-DBE}} = 6 \mu\text{L}$ in 5 mL).

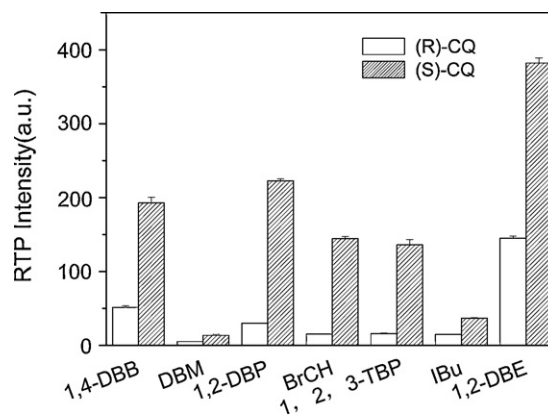


Fig. 3. Effect of different heavy atom perturbers on the RTP intensity of CQ in α -CD solution ($[\text{CQ}] = 1.0 \times 10^{-3} \text{ mol L}^{-1}$; $[\alpha\text{-CD}] = 2.0 \times 10^{-2} \text{ mol L}^{-1}$; $V_{\text{HAP}} = 6 \mu\text{L}$ in 5 mL).

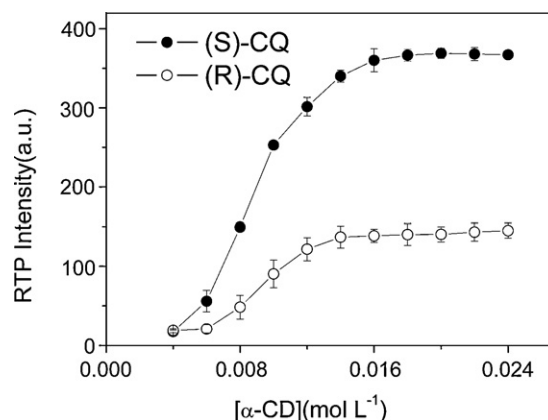


Fig. 4. Effect of α -CD concentration on the RTP intensity of CQ. ($[\text{CQ}] = 1.0 \times 10^{-3} \text{ mol L}^{-1}$; $V_{1,2\text{-DBE}} = 6 \mu\text{L}$ in 5 mL).

The variation in the RTP with 1,2-DBE concentrations is shown in Fig. 5. It can be seen that with the increase of 1,2-DBE, the RTP intensity increased and reached a maximum value when the volume proportion of 1,2-DBE in the working solution was more than 0.12% and then slightly decreased to a plateau. A suitable 1,2-DBE volume of 0.12% was selected in this work.

3.2.3. RTP of mixed (R)-CQ and (S)-CQ enantiomers

Under optimal conditions, RTP spectra obtained from mixtures of (R)- and (S)-CQ at different R/S ratios were shown in Fig. 6. As

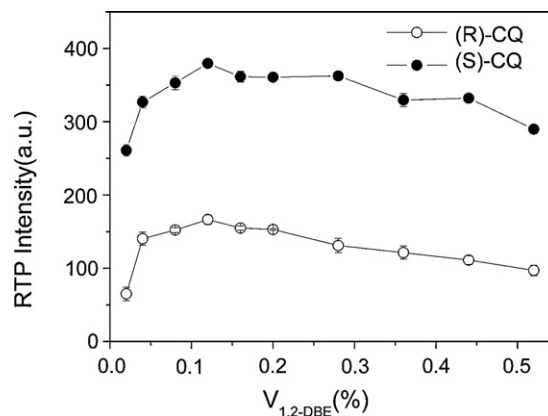


Fig. 5. Effect of the volume of 1,2-DBE on the RTP intensity of CQ. ($[\text{CQ}] = 1.0 \times 10^{-3} \text{ mol L}^{-1}$; $[\alpha\text{-CD}] = 2.0 \times 10^{-2} \text{ mol L}^{-1}$).

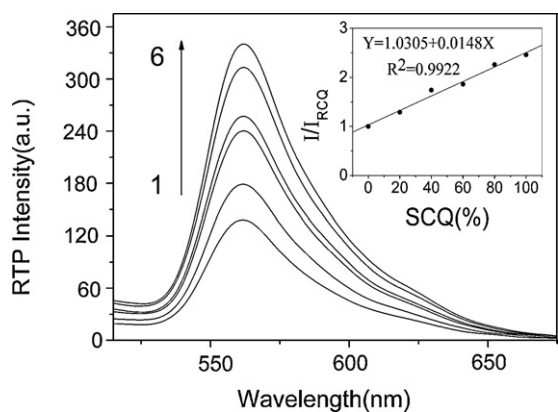


Fig. 6. RTP spectra of CQ at various S-compositions. ($[\alpha\text{-CD}] = 2.0 \times 10^{-2} \text{ mol L}^{-1}$; $V_{1,2\text{-DBE}} = 6 \mu\text{L}$ in 5 mL; $[(R)\text{-CQ}]/[(S)\text{-CQ}]$: (1) 1:0, (2) 4:1, (3) 3:2, (4) 2:3, (5) 1:4, (6) 0:1.) Inset: phosphorescence enhancement of CQ versus the enantiomeric composition of CQ.

is seen in the inset of Fig. 6, the RTP intensity can be correlated linearly with the enantiomeric composition of CQ. Therefore the proposed method enables the determination of the enantiomeric composition of a CQ mixture.

3.3. Complexation equilibria

The inclusion constants and the stoichiometries of the inclusion complexes were determined by a combination of absorption, fluorescence and phosphorescence measurements. Keeping the concentration of CQ constant, the changes in absorbance and emission upon addition of $\alpha\text{-CD}$ to the solution were measured and the data were analyzed in terms of formation of 1:1 and 1:2 complexes of CQ with $\alpha\text{-CD}$ by Benesi–Hildebrand plots. As shown in Fig. 7, the plot of $1/\Delta A$ (the reciprocal of the changes in absorbance at 454 nm) against $1/[\alpha\text{-CD}]$ (the reciprocal of the $\alpha\text{-CD}$ concentration) is bent upward and the plot of $1/\Delta A$ against $1/[\alpha\text{-CD}]^2$ is downward, indicating that the CQ: $\alpha\text{-CD}$ complexes of both 1:1 and 1:2 stoichiometry are formed. However, a good linear relationship obtained between $1/\Delta I$ (the reciprocal of the changes in fluorescence emission intensity at 500 nm (475 nm excitation)) and $1/[\alpha\text{-CD}]^2$, indicating that only the formation of the CQ: $\alpha\text{-CD}$ complex with 1:2 stoichiometry can produce considerable fluorescence emission intensity enhancement. Similar phosphorescence emission changes were observed. The plot of $1/\Delta P$ (the reciprocal of the changes in phosphorescence emission intensity) against $1/[\alpha\text{-CD}]^2$ is linear (Fig. 7f) while the plot of $1/\Delta P$ against $1/[\alpha\text{-CD}]$ is bent upward (Fig. 7e). We can conclude that the formation of the ternary complex with the CQ: $\alpha\text{-CD}$ stoichiometry 1:2 results in

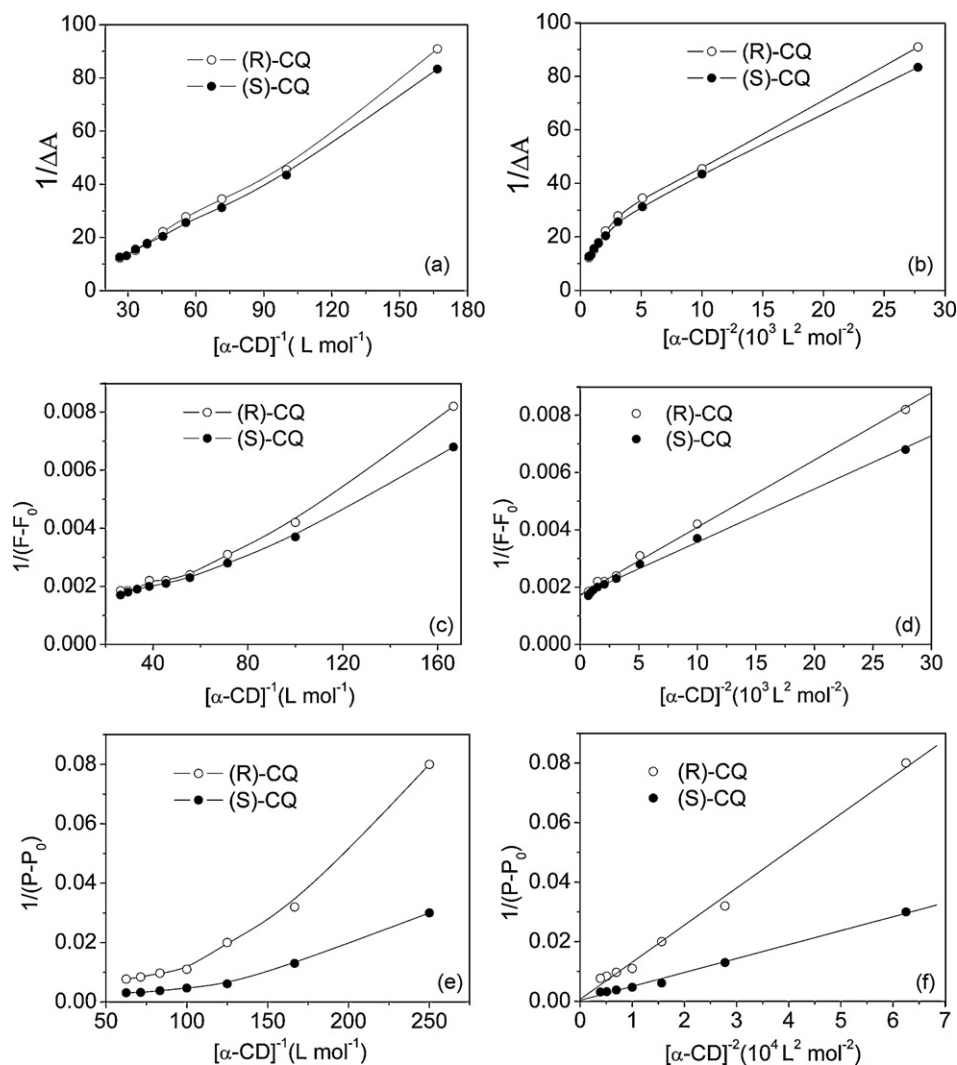
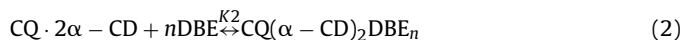


Fig. 7. Double reciprocal plots for (R)-CQ/ $\alpha\text{-CD}$ and (S)-CQ/ $\alpha\text{-CD}$ complexes constructed using absorption (a and b), fluorescence (c and d), and phosphorescence (e and f) data, assuming two different CQ: $\alpha\text{-CD}$ stoichiometries: 1:1 (a, c, and e) and 1:2 (b, d, and f). ($[\text{CQ}] = 1.0 \times 10^{-3} \text{ mol L}^{-1}$; $V_{1,2\text{-DBE}} = 6 \mu\text{L}$ in 5 mL for phosphorescence).

strong phosphorescence emission and the formation of the ternary complex with the CQ:α-CD stoichiometry 1:1 is at most a minor process. Assuming that a 1:2:n ternary complex CQ/α-CD/1,2-DBE is formed, the formation of the complex can be described by several equilibria:



The formation constants of the binary complex K_1 was first calculated from the fluorescence data by use of the following modified Benesi–Hildebrand equation [26].

$$\frac{1}{F - F_0} = \frac{1}{K[\alpha - \text{CD}]^2[F_\infty - F_0]} + \frac{1}{F_\infty - F_0} \quad (3)$$

where F is the observed fluorescence intensity of CQ solution at each α-CD concentration, F_0 presents fluorescence intensity of CQ solution in the absence of α-CD. The calculated formation constant K_1 are $(7.79 \pm 0.30) \times 10^3 \text{ L}^2 \text{ mol}^{-2}$ and $(9.21 \pm 1.55) \times 10^3 \text{ L}^2 \text{ mol}^{-2}$ for (R)-CQ and (S)-CQ, respectively, which corresponds to a diastereoisomer selectivity of ca. 1: 1.2.

When the concentrations of both α-CD and 1,2-DBE are much greater than that of CQ, their free and analytical concentrations are similar and therefore the mass balance for CQ can be written as:

$$C_{\text{CQ}} = [\text{CQ}](1 + K_1 C_{\text{CD}}^2 + K_1 K_2 C_{\text{CD}}^2 C_{\text{DBE}}^n) \quad (4)$$

where C_{CQ} , C_{CD} and C_{DBE} are the analytical concentrations of CQ, α-CD and 1,2-DBE, respectively, and $[\text{CQ}]$ is the free concentration of CQ.

If the RTP emission is predominantly from the triplet state ternary inclusion complex, then the increase in the intensity of phosphorescence should be proportional to the ternary complex concentration:

$$I_p - I_0 = m[\text{CQ} \cdot (\alpha - \text{CD})_2\text{DBE}_n] \quad (5)$$

where I_p and I_0 are the phosphorescence intensities of CQ in the presence and in the absence of 1,2-DBE, respectively; m is a proportionality constant. Assuming that at high 1,2-DBE concentrations essentially all of the CQ molecules are complexed, the following equation can be written:

$$I_{p\infty} - I_0 = mC_{\text{CQ}} \quad (6)$$

where $I_{p\infty}$ is the RTP intensity when the complex is completely formed. Combining Eqs. (4)–(6) gives:

$$I_p - I_0 = \left[\frac{K_1 K_2 C_{\text{CD}}^2 C_{\text{DBE}}^n (I_{p\infty} - I_0)}{1 + K_1 C_{\text{CD}}^2 + K_1 K_2 C_{\text{CD}}^2 C_{\text{DBE}}^n} \right] \quad (7)$$

when $1/I_p - I_0$ is plotted versus $1/[\text{1,2-DBE}]^2$, a good linear relationship is observed for both R-CQ and (S)-CQ systems. The values for K_2 , calculated from the ratio of the intercept to slope, are $(1.22 \pm 0.23) \times 10^5 \text{ L}^2 \text{ mol}^{-2}$ and $(3.39 \pm 0.56) \times 10^5 \text{ L}^2 \text{ mol}^{-2}$ for (R)-CQ and (S)-CQ, respectively. These overall association constant values are much higher than that for the binary complexes, indicating that 1,2-DBE largely enhanced the inclusion ability of α-CD with CQ. Moreover, the difference in the inclusion efficiency was much more pronounced for the two isomers in the presence of a third component. It can be concluded that the mobility of the (S)-CQ in α-CD cavity should be lower than that of the (R)-CQ in the presence of 1,2-DBE, suggesting that there is a more precise stereochemical matching between (S)-CQ and α-CD.

As is shown in the above discussion, the differences in the absorption and fluorescence spectra of the two CQ enantiomers in the presence of CDs (α-, β- or γ-CD) are too small to be used for chiral discrimination. By contrast, the CD-RTP can be easily detected in the presence of different third components, which can induce chirality discrimination and play a very important role in chirality manifestations.

3.4. Phosphorescence decay

The biexponential triplet decay of RCQ and SCQ enantiomers in an aqueous solution of $1 \times 10^{-2} \text{ mol L}^{-1}$ α-CD were previously reported by Bortolus et al. [3]. The lifetimes, determined by triplet-triplet absorption spectroscopy, were 5 ± 1 and $45 \pm 5 \mu\text{s}$ for (R)-CQ and 4 ± 1 and $55 \pm 5 \mu\text{s}$ for (S)-CQ, respectively. Moreover, the relative weight of the longer-lived component increased with the increase of CD concentration. The short-lived component was assigned to the free guest and/or to the 1:1 complex while the long-lived component was attributed to the 2:1 complex. In our case, the lifetimes of both (R)-CQ and (S)-CQ were determined by plotting the phosphorescence intensity against the delay time and different results were obtained. Both (R)-CQ and (S)-CQ displayed a mono-exponential phosphorescence decay, which is consistent with the results of the α-CD–CQ binary complexes reported by Gooijer and co-workers [16]. The observed mono-exponential phosphorescence decays further support the above interpretation, i.e., only the formation of the ternary complex with the CQ:α-CD stoichiometry 1:2 results in strong phosphorescence emission.

Fig. 8 shows the phosphorescence decay curves and the residual analysis for both (R)-CQ and (S)-CQ. The lifetimes of (R)-CQ and (S)-CQ are $(0.274 \pm 0.014) \text{ ms}$ ($R^2 = 0.99915$) and $(0.639 \pm 0.021) \text{ ms}$ ($R^2 = 0.99942$), respectively. The lowest excited triplet state of CQ has n, π^* character. So the lifetimes obtained here are shorter (sub-ms) than that previously observed for quinine and quinidine as well as 1,1'-binaphthol, which have lowest π, π^* triplet states and

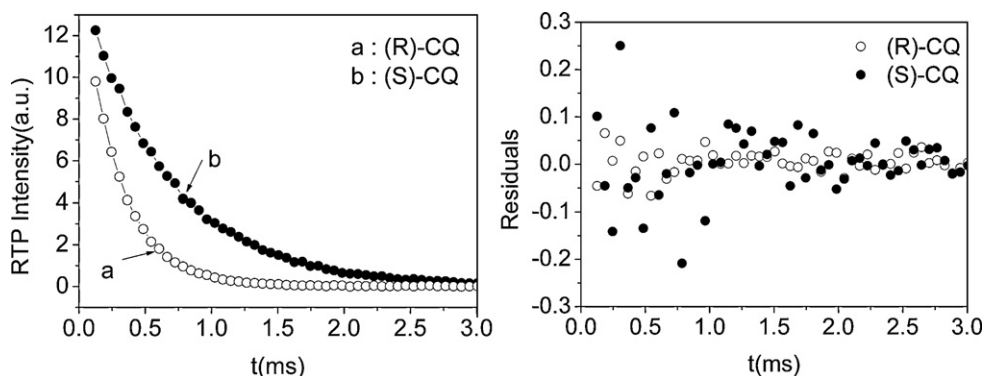


Fig. 8. (Left) Phosphorescence decay curves of (R)-CQ and (S)-CQ. (Right) Residual analysis of phosphorescence decay fitting of (R)-CQ and (S)-CQ. $[\text{CQ}] = 1.0 \times 10^{-3} \text{ mol L}^{-1}$; $[\alpha\text{-CD}] = 2.0 \times 10^{-2} \text{ mol L}^{-1}$; $V_{1,2\text{-DBE}} = 6 \mu\text{L}$ in 5 mL).

exhibited lifetimes in the ms range [18,19]. The lifetime difference between (R)-CQ and (S)-CQ is 80.0%, indicating a distinct chiral discrimination of α -CD toward this pair of enantiomers. Based on the observed RTP lifetime differences, time-resolved RTP technique can be used for the recognition of (R)-CQ and (S)-CQ without deoxygenation.

It should be noted that the triplet lifetimes of the CQ/1,2-DBE/ α -CD complexes are much higher than those of the α -CD–CQ binary complexes (0.352 ± 0.016 ms for (S)-CQ and 0.089 ± 0.006 ms for (R)-CQ) reported in deoxygenated medium [16]. Actually, the lifetime of (S)-CQ/1,2-DBE/ α -CD complex is closer to the value measured in poly(vinyl chloride) film (0.760 ms) [27], indicating that addition of a third component efficiently protected CQ in the CD cavity from the quenchers in bulk solution. According to the literature, the dissociation of the 2:1 α -CD–CQ binary complex to the 1:1 complex would reduce both the phosphorescence intensity and lifetime [3].

The dissociation rate constants for the two enantiomers, $k_D(R)$ and $k_D(S)$, can be calculated from the following equation:

$$\tau = \frac{1}{\tau_0^{-1} + k_D} \quad (8)$$

where τ_0 and τ are respectively phosphorescence lifetimes in the absence and in the presence of dissociation and k_D is the rate constant of dissociation. On the basis of the method proposed by Gooijer and co-workers [16], k_D can be estimated by considering two extreme cases. One is assuming that τ_0 is 0.430 ms, the highest triplet lifetime of CQ reported in organic solvents [25], and the other is assuming that dissociation plays no role for the (S)-enantiomer so that τ_0 is 0.352 ms, the value determined in their experiment. Since the lifetime of (S)-CQ determined in our experiment is larger than 0.430 ms, the difference in dissociation rates between (R)-CQ and (S)-CQ (Δk_D) can only be estimated by considering the latter case, i.e., assuming that dissociation plays no role for the (S)-enantiomer so that τ_0 is 0.639 ms, the value determined in our study. In this case, $k_D(S)$ is zero, while $k_D(R)$ is $2.1 \times 10^3 \text{ s}^{-1}$, and Δk_D is $2.1 \times 10^3 \text{ s}^{-1}$. This value is smaller than that in the α -CD–CQ binary complex ($8.4 \times 10^3 \text{ s}^{-1}$) [16], indicating that the ternary complexes are more stable with smaller dissociation rate constants so that the difference in dissociation rates between (R)-CQ/1,2-DBE/ α -CD and (S)-CQ/1,2-DBE/ α -CD ternary complexes is smaller than that in typical binary complexes. Thus, it can be interpreted that the lifetime difference between (R)-CQ and (S)-CQ in our study is somewhat less than that observed in deoxygenated medium (119%) [16].

3.5. NMR studies

For a better understanding of the interaction model of the ternary inclusion complex of CQ/1,2-DBE/ α -CD, ^1H NMR spectra in the mixed solvent of D_2O and CD_3COCD_3 with the volume proportion 20:1 were measured. CD_3COCD_3 was added in order to improve the CQ solubility. Chart 1 shows the numbering of carbon atoms in the α -CD glucopyranose residue [28]. The change of chemical shifts of protons in α -CD in the presence of CQ and 1,2-DBE are collected in Table 1. It can be seen that in the binary system of α -CD and CQ, $\Delta\delta_1$ of H-3, H-5 and H-6 displayed a larger change, and the other protons smaller. On the whole, the change of chemical shifts showed the following order: $\Delta\delta(\text{H-3}) \sim \Delta\delta(\text{H-6}) > \Delta\delta(\text{H-5}) > \Delta\delta(\text{H-2}) > \Delta\delta(\text{H-4}) \approx \Delta\delta(\text{H-1})$. Chemical shift changes in H-3 of α -CD are larger than those in H-5, indicating that the CQ molecule is included in the hydrophobic cavity at the wider end. In the ternary complex of CQ/1,2-DBE/ α -CD, significant upfield shifts for H-5 and H-6 were observed, whereas the change of H-3 is very similar to that of $\Delta\delta_1$. It can be inferred that 1,2-DBE molecule is introduced within α -CD

Table 1

^1H chemical shifts corresponding to α -CD in the presence of different components.

	δ_0 (ppm) ^a	$\Delta\delta_1$ ^a		$\Delta\delta_2$ ^a	
		(R)-CQ	(S)-CQ	(R)-CQ	(S)-CQ
H1	4.961	−0.001	−0.003	0.009	0.001
H2	3.529	−0.005	−0.005	0.024	0.019
H3	3.926	−0.063	−0.062	−0.058	−0.065
H4	3.499	−0.004	−0.004	0.027	0.018
H5	3.744	−0.044	−0.041	−0.063	−0.113
H6	3.895	−0.063	−0.061	−0.089	−0.097

^a δ_0 indicates the chemical shifts of protons in α -CD, and $\Delta\delta_i = \delta_i - \delta_0$ ($i = 1, 2$), where 1 and 2 correspond to the respective CD protons in solutions of α -CD + CQ and α -CD + CQ + 1, 2-DBE.

through the narrower end of the cavity. The lone electron pairs of the bromine atom of 1,2-DBE molecule may produce the shielding effects on H-5 and H-6, which induced their significant upfield shifts. It should be noted that the differences of $\Delta\delta_2$ between (R)-CQ and (S)-CQ are larger than that of $\Delta\delta_1$, indicating that the addition of 1,2-DBE as a third component plays an important role in the chiral recognition of α -CD to the CQ enantiomers. It can be inferred that the addition of 1,2-DBE leads to reorganization in the host–guest interactions and the complex structures are not identical for the binary and the ternary complex.

^2D NMR spectroscopy has also been used to study the inclusion complexation of α -cyclodextrin with CQ in order to understand the binding model. Fig. 9 shows a spatial contour plot of the ROESY spectrum for the (S)-CQ/ α -CD system. Relatively strong interactions of the H-8', H-9' and H-10' with the cyclodextrin protons were observed, whereas only weak interactions of the H-4' and H-5' protons with the cyclodextrin protons were observed. No cross-peak was detected for H-6' in CQ. This indicates that (S)-CQ inserts into the hydrophobic cavity of cyclodextrin with the hydrophobic part and the H-8', H-9' and H-10' part of the molecule is deeply included inside the CD cavity. On the basis of the spectroscopic as well as the NMR results, the inclusion structure of CQ/1,2-DBE/ α -CD is illustrated in Fig. 10. In the presence of α -CD, the H-8', H-9' and H-10' part of the CQ molecule penetrates into the polar cavity from the more accessible wider side of CD. But a part of the CQ molecule

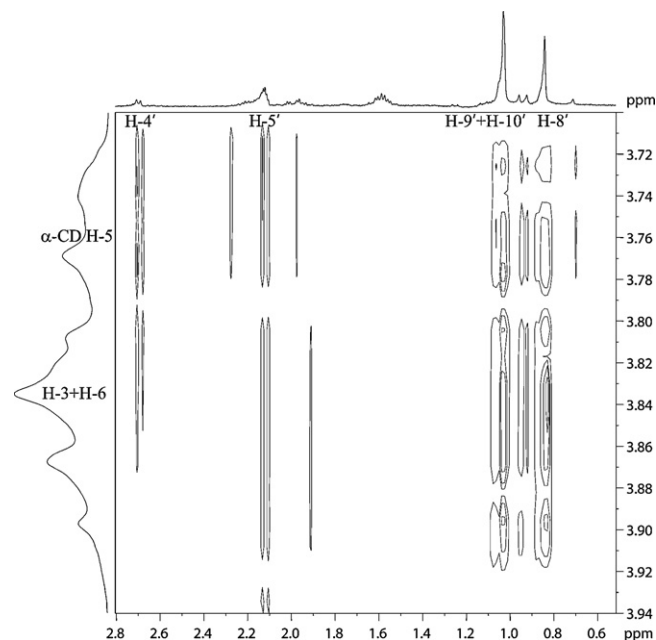


Fig. 9. Partial contour plot of a ROESY spectrum of α -CD/(S)-CQ complex at 25 °C. (300 MHz, $\text{D}_2\text{O}/\text{CD}_3\text{COCD}_3$ 20:1).

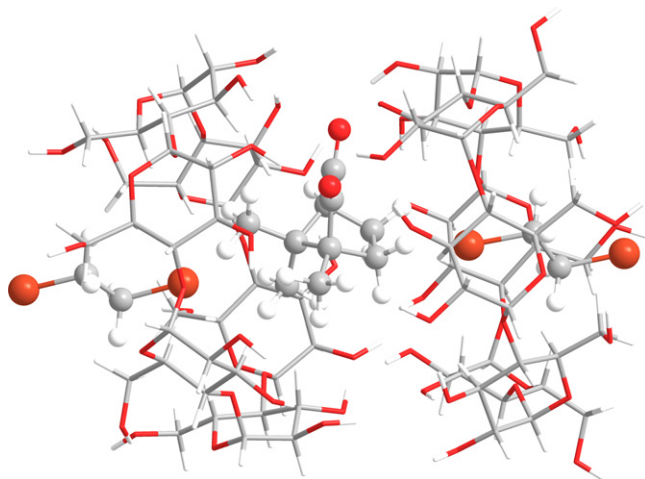


Fig. 10. Schematic representation showing the inclusion model of the CQ/1,2-DBE/ α -CD complex.

containing H-4' and H-5' is located outside the cavity, which can then be enclosed by a second cyclodextrin to give a complex in a 1:2 stoichiometric ratio. 1,2-DBE, acting as a space-filling component, inserts into the hydrophobic cavity of cyclodextrin from the narrower opening and forms a stable tertiary complex, namely, CQ/1,2-DBE/ α -CD.

4. Conclusions

When camphorquinone is included in cyclodextrin molecules in the presence of a heavy atom moiety such as 1,2-dibromoethane, it exhibits strong and stable room temperature phosphorescence (RTP) emissions. Moreover, the CQ/1,2-DBE/ α -CD complexes exhibit enantiomeric differentiation in both RTP intensity and RTP lifetime, enabling easy spectroscopic discrimination between (R)-CQ and (S)-CQ enantiomers based on simple time-resolved detection. The RTP intensity can be correlated linearly with the enantiomeric composition of CQ, which enables the determination of the enantiomeric composition of a CQ mixture. ^1H NMR as well as 2D NMR spectroscopic studies show that the CQ molecule is included in the hydrophobic cavity at the wider end while 1,2-DBE molecule is introduced within α -CD through the narrower end of the cavity.

Acknowledgments

This work was financially supported by the National Natural Science Foundation of China (no. 20675009), the Natural Science Foundation of Shanxi Province (no. 2008011015-1) and the project sponsored by Shanxi Province for the Returned Overseas Chinese Scholars (2007).

References

- [1] M.V. Rekharsky, H. Yamamura, M. Kawai, Y. Inoue, Complexation and chiral recognition thermodynamics of γ -cyclodextrin with *N*-Acetyl- and *N*-carbobenzoyloxy-dipeptides possessing two aromatic rings, *J. Org. Chem.* 68 (2003) 5228–5235.
- [2] P. Skowronek, J. Ścianowski, J. Gawroński, Helicity discrimination in diselenides by chiral substituents—a circular dichroism study, *Tetrahedron: Asymmetry* 17 (2006) 2408–2412.
- [3] P. Bortolus, G. Marconi, S. Monti, Chiral discrimination of camphorquinone enantiomers by cyclodextrins: a spectroscopic and photophysical study, *J. Phys. Chem. A* 106 (2002) 1686–1694.
- [4] W.A. Tao, F.C. Gozto, R.G. Cooks, Mass spectrometric quantitation of chiral drugs by the kinetic method, *Anal. Chem.* 73 (2001) 1692–1698.
- [5] B. Merelli, M. Carli, L. Menguy, J.C. Cherton, Enantiomeric composition of chiral beta-hydroxylamides by ^1H NMR spectroscopy using chiral solvating agent, *Spectrosc. Lett.* 41 (2008) 361–368.
- [6] B.C. Valle, K.F. Morris, K.A. Fletcher, V. Fernand, D.M. Sword, S. Eldridge, C.K. Larive, I.M. Warner, Understanding chiral molecular micellar separations using steady-state fluorescence anisotropy, capillary electrophoresis, and NMR, *Langmuir* 23 (2007) 425–435.
- [7] A.M. Costeroa, M. Colera, P. Gaviña, S. Gil, M. Kubinyi, K. Pál, M. Kállay, Chiral cyclohexane based fluorescent chemosensors for enantiomeric discrimination of aspartate, *Tetrahedron* 64 (2008) 3217–3224.
- [8] A. Cavazzini, G. Nadalini, F. Dondi, F. Gasparini, A. Cioqli, C. Villani, Study of mechanisms of chiral discrimination of amino acids and their derivatives on a teicoplanin-based chiral stationary phase, *J. Chromatogr. A* 1031 (2004) 143–158.
- [9] S. Li, W.C. Purdy, Cyclodextrins and their applications in analytical chemistry, *Chem. Rev.* 92 (1992) 1457–1470.
- [10] Y. Liu, L. Li, H.Y. Zhang, Z. Fan, X.D. Guan, Selective binding of chiral molecules of cinchona alkaloid by β - and γ -cyclodextrins and organoselenium-bridged bis(β -cyclodextrin)s, *Bioorg. Chem.* 31 (2003) 11–23.
- [11] H. Bakirci, W.M. Nau, Chiral discrimination in the complexation of heptakis-(2,6-di-*O*-methyl)- β -cyclodextrin with 2,3-diazabicyclo[2.2.2]oct-2-ene derivatives, *J. Photochem. Photobiol. A: Chem.* 173 (2005) 340–348.
- [12] B.D. Wu, Q.Q. Wang, L. Guo, R. Shen, J.W. Xie, L.H. Yun, B.H. Zhong, Amino-substituted β -cyclodextrin copper(II) complexes for the electrophoretic enantioseparation of dansyl amino acids: Role of dual chelate–inclusion interaction and mechanism, *Anal. Chim. Acta* 558 (2006) 80–85.
- [13] V. Pavan Kumar, I. Suryanarayana, Y.V.D. Nageswar, K. Rama Rao, Chiral discrimination of tolterodine tartrate by modified cyclodextrins, *J. Carbohydr. Chem.* 27 (2008) 223–230.
- [14] C. García-Ruiz, X.S. Hu, F. Ariese, C. Gooijer, Enantioselective room temperature phosphorescence detection of non-phosphorescent analytes based on interaction with β -cyclodextrin/1-bromonaphthalene complexes, *Talanta* 66 (2005) 634–640.
- [15] Y.L. Wei, W.H. Chan, A.W.M. Lee, C.W. Huie, Alteration of room temperature phosphorescence lifetimes of quinine and quinidine by chiral additives, *Chem. Commun.* (2004) 288–289.
- [16] C. García-Ruiz, M.J. Scholtes, F. Ariese, C. Gooijer, Enantioselective detection of chiral phosphorescent analytes in cyclodextrin complexes, *Talanta* 66 (2005) 641–645.
- [17] Y.L. Wei, C. Dong, D.S. Liu, S.M. Shuang, C.W. Huie, Enantioselective quenching of room-temperature phosphorescence lifetimes of proteins: bovine and human serum albumins, *Biomacromolecules* 8 (2007) 761–764.
- [18] X.H. Zhang, Y. Wang, W.J. Jin, Chiral discrimination of quinine and quinidine based on notable room temperature phosphorescence lifetime differences with γ -cyclodextrin as chiral selector, *Talanta* 73 (2007) 938–942.
- [19] X.H. Zhang, Y. Wang, W.J. Jin, Enantiomeric discrimination of 1,1'-binaphthol by room temperature phosphorimetry using γ -cyclodextrin as chiral selector, *Anal. Chim. Acta* 622 (2008) 157–162.
- [20] I. Lammers, J. Buijs, G. van der Zwan, F. Ariese, C. Gooijer, Phosphorescence for sensitive enantioselective detection in chiral capillary electrophoresis, *Anal. Chem.* 81 (2009) 6226–6233.
- [21] S. Scypinski, L.J. Cline Love, Room-temperature phosphorescence of polynuclear aromatic hydrocarbons in cyclodextrins, *Anal. Chem.* 56 (1984) 322–327.
- [22] H.H. Alvim, A.C. Alecio, W.A. Vasconcellos, M. Furlan, J.E. de Oliveira, J.R.C. Saad, Analysis of camphorquinone in composite resins as a function of shade, *Dent. Mater.* 23 (2007) 1245–1249.
- [23] M.-H. Chen, C.-R. Chen, S.-H. Hsu, S.-P. Sun, W.-F. Su, Low shrinkage light curable nanocomposite for dental restorative material, *Dent. Mater.* 22 (2006) 138–145.
- [24] A. Romani, G. Favaro, F. Masetti, Luminescence properties of camphorquinone at room temperature, *J. Lumin.* 63 (1995) 183–188.
- [25] C.E. Dalglish, The optical resolution of aromatic amino acids on paper chromatograms, *J. Chem. Soc.* 137 (1952) 3940–3942.
- [26] X.H. Wen, F. Tan, Z.J. Jing, Z.Y. Liu, Preparation and study the 1:2 inclusion complex of carvedilol with β -cyclodextrin, *J. Pharma. Biomed. Anal.* 34 (2004) 517–523.
- [27] J.M. Charlesworth, T.H. Gan, Kinetics of quenching of ketone phosphorescence by oxygen in a glassy matrix, *J. Phys. Chem.* 100 (1996) 14922–14927.
- [28] N. Fatin-Rouge, J.-C.G. Bünzli, Thermodynamic and structural study of inclusion complexes between trivalent lanthanide ions and native cyclodextrins, *Inorg. Chim. Acta* 293 (1999) 53–60.